Tellus (1992), *44A*, 41–53

Comparison of two parameterization schemes for cloud and precipitation processes

By FRODE FLATØY, *Department of Geophysics, University of Bergen, Allegaten 70, N-5007 Bergen, Norway*

(Manuscript received 19 November 1990; in final form 8 August 1991)

ABSTRACT

Two parameterization schemes for cloud and precipitation formation, by Kessler and Sundqvist respectively, are described, and compared while simulating various atmospheric conditions. To do this, a simple one-dimensional numerical model is used. The effect of changes in parameter values in the two schemes are studied, and it is shown that Sundqvist's and Kessler's schemes, when used on the same cases and with a suitable choice of parameters, give results with good correspondence with each other. Results from the calculations are also compared with available measurements. The results demonstrate that the simpler Sundqvist scheme is suitable for implementation in a numerical weather prediction model.

1. Introduction

The treatment of condensation and cloud processes in numerical weather prediction models (NWP) and global climate models (GCM) is indeed simplified. However, not least because many models contain radiation calculations, it appears that more advanced handling of such processes will gradually be common features of the models. Charlock (1982) and Charlok and Ramanathan (1985), have pointed that the cloud water content has an important impact on the resulting radiative transfer. Roeckner et al. (1987) has demonstrated this importance in climate model integration.

In order to make clouds appear in connection with the condensation, it is necessary to partition the condensate between cloud water and precipitating water. This implies that micro-physical processes have to be accounted for. The inclusion of cloud micro-physics is a field that so far has been neglected in many models. The research model developed by Sundqvist et al. (1989) has given results in specific cases that demonstrate the importance of including the cloud and rain processes in a proper manner. The problem is how the knowledge we already have in cloud microphysics should be applied in NWP/GCM models. It is clear that the incorporation of such processes has to be done with the aid of a parameterization scheme.

Today essentially two such schemes are in use in large scale models, one suggested by Kessler (1969) and one by Sundqvist (1988). The Kessler parameterization scheme (Ks) is built directly on the known micro-physical processes. The scheme contains one term for each process and both cloud water and precipitating water are prognostic variables. With regard to the detailed treatment, the vertical resolution ought to be rather high for consistency. Thereby it is an expensive scheme to use when the computing time is important. Sundqvist's scheme (Sq) has another philosophy, as it contains only one term and only one prognostic variable, the cloud water content. This reflects the fact that the parameterization was developed for use in a prediction model from the start, and not as with (Ks) created for studying the microphysical processes in more detail. The aim of this study is to investigate how (Sq) can be used under different conditions, and point to possible weaknesses in it. To do this, we have used the results obtained with (Ks) as a reference, performing the same computations with both schemes. The idea is to use the models to find realistic values for the different parameters under varying conditions.

In order to adjust the parameterizations to behave realistically, it is desirable, if not necessary, to have available measurements of cloud water amount as a function of height, and of the corresponding precipitation at ground level. However, it has not been possible to find measured profiles of cloud water content. Statistical data of cloud water amount, at different temperatures may be found from Matveev (1984). But those data, being mean values from a great number of samples, can only be used to indicate if the model results are reasonable. The two schemes will be compared with each other and the model results will be examined to see if they are realistic, when compared to the sparse existing measurements. We first study the sensitivity of the results of the individual schemes to variations in parameter values (section 4.2). Then we compare the two schemes under various forcings simulating different atmospheric conditions (sections 4.3–4.5). We have done this numerically, but it can also be done analytically as demonstrated for Kesslers scheme by Heiden and Kahlig (1988). Results about how the schemes behave in a NWP model is not presented here, but can be found in Sundqvist et al. (1989) or Kristjànson (1991).

2. The parameterization schemes

2.1. *The Kessler scheme*

In his approach, Kessler (1969) considered both cloud water m and precipitation water M as prognostic variables. He introduces the quantity m through the following definition: $m = \pi - Q_s + Q$, where π is the specific cloud water content, Q_s the specific saturation vapour content and Q the actual specific vapour content. Then when m is positive, m is the amount of cloud water, and the actual vapour content equals the saturation vapour content. When m is negative, the cloud content is zero, and $|m|$ is the amount of moisture required to saturate the air. The equations for M and m, in terms of specific water content (kg/kg), are

$$\frac{\partial M}{\partial t} = -(w + V)\frac{\partial M}{\partial z} - M\left(\frac{\partial V}{\partial z} + V\frac{\partial \ln \rho}{\partial z}\right) + P(z), \tag{2.1}$$

$$\frac{\partial m}{\partial t} = -w\frac{\partial m}{\partial z} + Q(z) - P(z). \tag{2.2}$$

Since we are only studying the equations in the vertical, the horizontal advection terms are omitted.

$Q(z) = wG$ is the condensation of water vapour and G is defined as

$$G = -\frac{\partial Q_s}{\partial z}. \tag{2.3}$$

We will study the bulk effect of interactions between the cloud and precipitation particles, and with the use of basic cloud physics, Rogers (1979), we can list the three terms representing the most important microphysical processes.

(a) Growth by diffusion, which we call autoconversion (AC) of cloud. This term describes the process of coalescence of cloud particles to form precipitation size particles.

(b) Growth of precipitation by collection within the cloud, called collision-coalescence (CC). When precipitation particles have formed their fall speed carries them through the cloud, and a growth of the precipitation particles through collection of cloud particles takes place.

(c) Evaporation of precipitation in unsaturated air (EP).

The microphysical terms can then symbolically be written as $P(z) = \mathrm{AC} + \mathrm{CC} - \mathrm{EP}$.

In the parameterization suggested by Kessler (1969), he distinguishes between the two precipitation forming processes in the following manner. The diffusion term (AC) is given as

$$\mathrm{AC} = k_1(m - a) \qquad \begin{array}{ll} k_1 > 0 & \text{when } m > a, \\ k_1 = 0 & \text{when } m < a, \end{array} \tag{2.4}$$

where a is the cloud water amount necessary for the onset of production of precipitation particles. Below this threshold value, auto conversion does not occur. The parameter k_1 gives the rate at which this transformation takes place.

For the parameterization of the collision-coalescence (CC) process, Kessler says that the terminal velocity of individual hydrometeors is proportional to the square root of the diameter. Applying the Marshall–Palmer (M–P) drop size distribution to the precipitation water content M, an average fall speed can be derived.

$$V(z) = -90{,}82\, N_0^{-1/8} \rho(z)\, M^{1/8}. \tag{2.5}$$

When assuming that (2.5) is valid, Kessler formulates an equation for the rate of change of the mass of a particle falling at speed V and sweeping out a cross-sectional area $\pi \rho_w D^2/4$. He than uses the M–P drop size distribution to formulate an expression for the collection of cloud by size-distributed rain

$$\frac{\delta M_i}{\delta t} = -\frac{\pi D_i^2}{4} E_i V_i m, \tag{2.6}$$

where E_i is the average efficiency with which the cloud particles of total mass m per unit mass of air are caught. Finally after integrating over all the particles, and adapting an average E which is independent over all D, the term describing coalescence becomes

$$\dot{CC} = k_2 E m M^{7/8} \rho(z). \tag{2.7}$$

This term is a function of both cloud water m and precipitation water M, and as a consequence it will only be of importance when rain water already exists at a level. This means that we can have release of precipitation at a level, even if m does not exceed a in the diffusion-term, because existence of rain water at a level can result from precipitation formed at higher levels. It follows from (2.5) that the constant k_2 in (2.7) is a function of N_0, the number of drops in the Marshall–Palmer drop size distribution, in the following way: $k_2 = k_2'(10^3 \rho_0)^{7/8} N_0^{1/8}$, $k_2' = 6.96 \cdot 10^{-4}$. As pointed out by Kessler k_2 is fairly insensitive to uncertainty in N_0, since the latter is raised the power $\frac{1}{8}$. The detailed, physically realistic description of release of precipitation and the inclusion of rain water as a prognostic variable makes this scheme more complex to use and more difficult to implement in a prediction model. Kessler's parameterization for the evaporation of precipitation will be studied in subsection 4.5.

2.2. *The Sundqvist scheme*

This parameterization was first suggested in Sundqvist (1978), and revised in Sundqvist (1988). In his parameterization, all rain water forming processes are incorporated in the term P (P = AC + CC):

$$P = C_0 m \left[1 - \exp\left(-\frac{m^2}{m_r^2}\right)\right], \tag{2.8}$$

where m is the specific cloud water content, m_r has a function similar to a in (2.4) and where the change in cloud water is a function only of the cloud water itself. Instead of including the rain water content as a prognostic variable, the CC effect is simulated with a modification of the parameters m_r and C_0.

$$m_r = \frac{m_{r0}}{F_1}, \tag{2.9}$$

$$C_0 = C_{00} F_1, \tag{2.10}$$

with the use of

$$F_1 = 1 + C_1 \tilde{P}^{0.5}, \qquad \tilde{P} = {}_h\int^H \rho P \,\mathrm{d}z, \tag{2.11}$$

with $C_1 \approx 100$, according to Sundqvist (1988). P is the rate of production of precipitation water at a single level, and $\tilde{P}$ is the rate of precipitation (kg m^{-2} s^{-1}) obtained by integration from the top of the model and down to the level in consideration. F_1 or C_1 has the corresponding effect as E in (2.7) of (Ks) and a term similar to (2.7) is thus introduced when C_1 is non-zero. In order to compare the two schemes correctly the rain water content M is included as a passive variable, dependent solely on the change in cloud water content expressed as $\partial M/\partial t = -\partial m/\partial t$. The (Sq) scheme is not as physically detailed as (Ks), but there are advantages. When the microphysics are incorporated in one term, and the rain water content no longer is a prognostic variable, the calculations are less complicated and less time consuming.

2.3. *Conditions of the model atmosphere*

We have employed a one-dimensional model in which either (Ks) or (Sq) is used to simulate the microphysical processes. The model's cloud base is at ground level, and condensation is assumed to form in saturated updrafts at a rate proportional to the updraft speed times the vertical gradient of saturation mixing ratio (2.14). The vertical wind at each level is constant (2.13), and thereby the production rate of condensate is constant in time. As the cloud water amount builds up, the production of precipitation water starts, and after some time steady-state is reached. During this process, the cloud/precipitation-profiles will show different shapes depending on the parameters. The time needed to reach steady-state, as well as the amount of cloud water at each level, are of course also functions of these parameters. In examples where unsaturated air occurs at some levels, precipitation is assumed to evaporate at a rate proportional to the subsaturation of the air (section 4.5). In all calculations in this paper, the atmosphere has a density ρ defined as

$$\rho = \rho_0 e^{kz}, \tag{2.12}$$

where $\rho_0 = 1.275$ kg/m^3 and $k = -10^{-4}$.

The profile of the updraft velocity has a parabolic shape, based on observations by Sulakvelidze(1969),

$$w = \frac{4w_{\max}}{H}\left(z - \frac{z^2}{H}\right). \tag{2.13}$$

In this study, we will treat cases with two different values of $w_{\max}$, $w_{\max} = 0.1$ m/s and $w_{\max} = 0.5$ m/s. Like Kessler, we assume a condensation function (2.3), decreasing with z:

$$G = A - Bz \ (\mathrm{m}^{-1}). \tag{2.14}$$

A typical condensation rate in the lower troposphere is found with $A = 3 \cdot 10^{-6}$ and $B = 3 \cdot 10^{-10}$.

3. Numerical considerations and model design

The finite difference form of the continuity equations follows the suggestion by Lax (1954) and is, with one exception, similar to the one used by Kessler (1969). Instead of using a centred finite difference scheme an upstream finite difference scheme is used; the reason for this will be explained later. The finite difference formulations of (2.1) and (2.2) are used where $P(z)$ contains the microphysical terms, that is, (2.8) when Sundqvist's scheme is applied and (2.4) plus (2.7), when Kessler's scheme is applied. C_0 and m_r are given in (2.9) and (2.10) and are dependent of the elevation z.

In all calculations, $|V| > w$, which assures that the finite difference formulation is upstream. The choice of Δt is dependent on the choice of Δz through the classical stability criteria, $\Delta t < (\Delta z / |-V + w_{\max}|)$ and $\Delta t < (\Delta z / |w_{\max}|)$.

Kessler calculates values for cloud and rain water content at time $t+1$ as a function only of the values at time t, which introduces a possibility for a systematic error. In the present study, the values of m at time $t+1$, have been computed as a function of the values at time t and $t+1$. When $m(z, t+1)$ is calculated implicitly instead of explicitly, the systematic error is reduced to a negligible value. In the model, this calculation is handled by an iteration-loop. When a centred finite difference scheme is applied, unstable oscillations are produced during the iteration procedure. These oscillations are effectively suppressed in the upstream finite difference scheme. The iteration procedure used is a Newton–Raphson type scheme.

Fig. 1 shows the temporal precipitation intensities from (Ks), with implicit and explicit solutions ($\Delta t = 30$ s). It is clearly seen that the two profiles are quite different. With implicit computation and iteration, the over-shooting (i.e., the peak in precipitation intensity) is reduced, and the convergence is slightly faster and smoother. The over-shooting is a consequence of the model formulation, and can be realistic in principle. But, since the magnitude is difficult to determine, the use of implicit computation is beneficial in order to suppress oscillations. From the corresponding profiles of (Sq), also shown in Fig. 1, we see that the two cases are virtually identical, implying that the influence of implicit computation on the Sundqvist scheme is negligible. However, for a longer time step the implicit time scheme may be preferable even in (Sq).

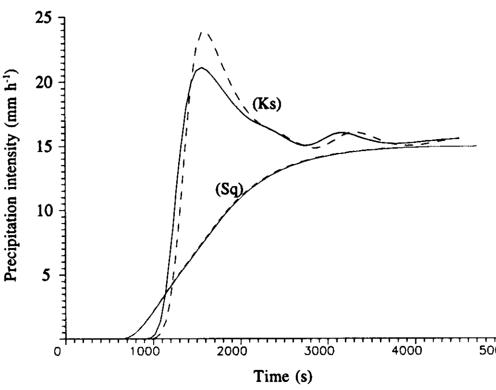

Fig. 1. Temporal changes in precipitation intensity in model runs with the two parameterizations. Dashed lines without iteration, solid lines with iteration.

4. Comparison of the two parameterization schemes

4.1. Basic considerations and establishment of a reference case

A number of test runs have been done to investigate what influence vertical advection has on the profiles of cloud and rain water and on the total water budget. The results presented in this section are computed when using (Sq). But a similar test has also been done with (Ks), giving almost identical results. Fig. 2 shows profiles of cloud water and rain water content at steady-state conditions for two cases with different sets of parameters: Case 1: $m_r = 2 \cdot 10^{-3}$, $C_{00} = 1.4 \cdot 10^{-3}$, $C_1 = 100$, Case 2: $m_r = 5 \cdot 10^{-3}$, $C_{00} = 1.0 \cdot 10^{-4}$, $C_1 = 150$. The two cases are chosen in order to get one situation with much cloud water, and one with little. The figure shows that in case 2, with much cloud water present, the inclusion of advection has a limited influence on the outline of the profiles. In case 1 the effect is negligible. We see that incorporation of vertical advection in some cases can yield important modification of cloud and rain water profiles as well as of precipitation intensity profiles. The latter is not shown but it can be seen from Fig. 2 that the precipitation rate at ground varies slightly with the choice of parameters. It is found that a loss occurs between the cloud and rain water phase. Kessler explains this discrepancy by the statement, that in a case with more cloud, "more condensate remains as cloud aloft and is spread horizontally by high-level divergence of the wind" (Kessler, 1969, p. 40). However, this can not be correct since the model is one dimensional and thus has no horizontal divergence. Instead it must be a result of the approximations in the continuity equations which induce a small artificial sink. Increasing the vertical resolution is a way to reduce the problem and in the next section it will be shown that an increasing spatial resolution has the result that the precipitation and production rates approach the same values.

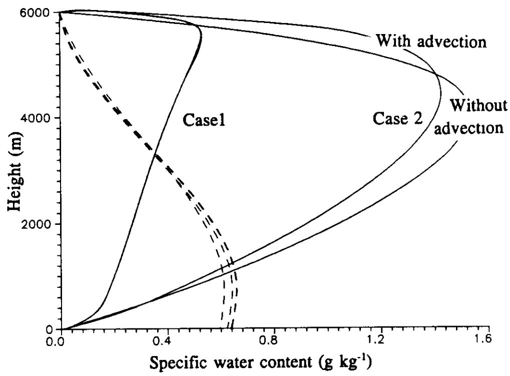

Fig. 2. Steady state profiles with/without advection for two sets of parameter values. Cloud water solid lines, rain water dashed lines. In case 1 the effect of advection is small and the two profiles are almost identical.

4.1.1. The spatial resolution. In this section, all the presented results are obtained with Kessler's scheme. A similar investigation with the Sundqvist scheme, showed that this is less sensitive to changes in the vertical resolution, and that hence results obtained with a coarse resolution were close to those obtained with a high one. Returning to (Ks) we examine how the choice of resolution influences the computed values. Three runs are made with different number of levels to indicate the effect the resolution has on the calculations. The first example is calculated with 40 levels, and the two others with 15 and 8 levels. Table 1 indicates the results. In the tabulated runs the parameters are $a = 0.5$, $k_1 = 0.01$ and $E = 1$. The choice of k_1 is only of importance during the onset of rain since $m < a$ (thus the AC-term equals 0) in most cases in a mature precipitating cloud. Steady-state conditions are assumed to be reached after 4500 s, and the production of condensed water is

Table 1. *Results for different vertical resolution when steady-state conditions are reached*

Levels		8	15	40	∞
Length of time step	(s)	120	60	20	—
Production rate cloud water	(mm h^{-1})	14.88	15.05	15.11	15.12
Production rate rain water	(mm h^{-1})	14.43	14.52	14.60	—
Precipitation rate	(mm h^{-1})	14.00	14.14	14.34	—

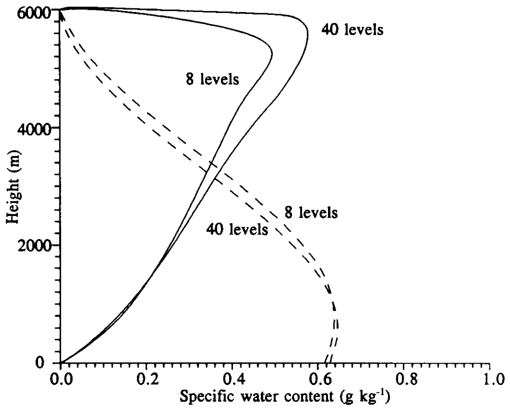

Fig. 3. Steady state cloud and rain water content from two calculations with 8 and 40 levels. Cloud water solid lines, rain water dashed lines.

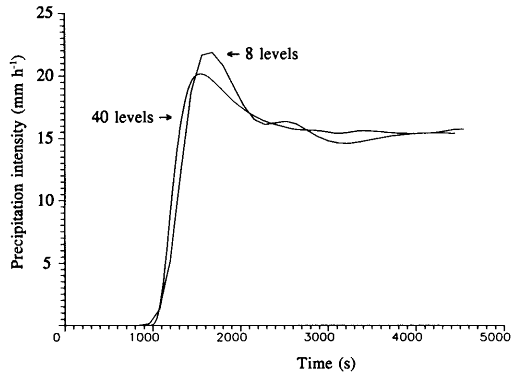

Fig. 4. Temporal variation of precipitation intensity for two model runs with 8 and 40 levels when (Ks) is used.

constant in time, given by (2.13) and (2.14). When the production-function is integrated analytically, the precise production is equivalent to a rainfall rate of 15.12 mm/h. At steady-state, the production rate of cloud water, the production rate of rain water, and the precipitation rate should in theory be identical, but from the table we see that this is not the case.

All quantities are dependent on the vertical resolution, and we see that when the number of levels is increased to 40, the results are still far from being in balance when the whole water budget is considered. Figs. 3–4 show results from the calculations presented in Table 1. Profiles of the cloud and rain water content are shown in Fig. 3. It shows that when the number of levels is increased, the total cloud water amount increases and the level of maximum is shifted upwards, while the rain water amount experiences a decrease at the upper levels and a slight increase at ground. As in the Table 1, Fig. 4 shows that the precipitation rate at steady-state approaches a higher value when the resolution is increased. The number of levels has also an effect on the smoothness of the approach to the steady-state value. We see that the convergence is smooth and fast in the 40-level case, while in the 8-level case, the oscillations are rather strong and the overshooting large. Several aspects have to be considered when one shall chose which resolution to use. A model with a high spatial resolution is of course the best when the accuracy of the results is the most important. The results presented later have all been worked out with a 15-level model, which has a short computing time and a sufficient accuracy in the present context. In a numerical weather prediction model, the number of levels usually is between 10 and 20. Therefore the accuracy of the results obtained with the 15 level model, is close to what one can expect when the scheme is implemented in a prediction model.

4.2. *Sensitivity for changes in the parameter values*

We shall first study the sensitivity of the reference case to changes in parameter values. All calculations in this chapter are made without vertical advection of cloud and rain water.

4.2.1. *The Kessler scheme.* The sensitivity to different values of the collision/coalescence-efficiency E is demonstrated in Kessler (1969). As could be expected the collision/coalescence effect influences both the integrated amount of cloud

Table 2. *Integrated cloud and rain water content for different E, C_1, C_∞ and m_{r0} (mm)*

	E				C_1				C_∞				m_{r0}			
	1.00	0.70	0.40	0.00	800	600	300	200	10^{-3}	$5\cdot10^{-4}$	$3\cdot10^{-4}$	$1.8\cdot10^{-4}$	10^{-4}	10^{-3}	$3\cdot10^{-3}$	$5\cdot10^{-3}$
Cloud water	1.71	2.23	3.13	6.77	1.33	1.75	3.32	4.74	0.92	1.71	2.80	4.65	1.67	1.87	3.03	4.07
Rain water	2.46	2.46	2.48	2.57	2.58	2.58	2.58	2.57	2.58	2.58	2.58	2.57	2.58	2.58	2.58	2.58

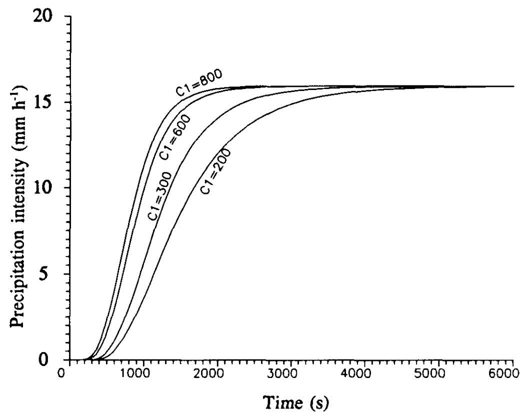

Fig. 5. Temporal variation of precipitation intensity at ground when C_1 varies and C_∞ and m_{r0} are constant.

water and the vertical distribution. The integrated cloud water amount decreases with increasing E, and the level of maximum is shifted upwards. One important point is that the overshooting preceding the steady-state increases with increasing values of E. For $E=0$, the convergence is very smooth, as expected, when only one of the micro-physical terms is active (This is qualitatively a simplified version of The Sundqvist scheme.). Table 2 gives the integrated cloud water and rain water content for a few profiles obtained with different E values. It is shown that the rain water content for $E=0$ is substantially larger than for larger values of E.

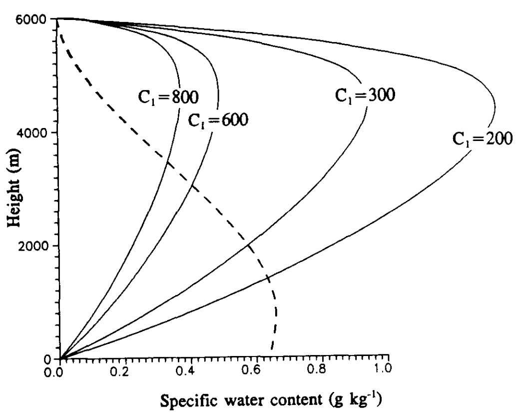

Fig. 6. Steady state cloud (solid lines) and rain (dashed lines) water profiles for different values of C_1.

This is due to the decreasing conversion rate as E decreases. Changes in k_1 and a will of course have other effects on the results. If a is increased it will lead to a time delay in the onset of rain, and cause the altitude at which the auto conversion term becomes zero to increase. If k_1 is increased a faster development towards steady-state conditions follows. Here we just refer to Kessler (1969), where the sensitivity in the results from changes in k_1 and a are clearly demonstrated. Satellite measurements, from McMurdie and Katsaros (1985), show that the integrated water content in a vertical cloud of this type very seldom is higher than 1.5 mm of liquid water. The high values in Table 2 are probably unrealistic, but they are shown to better demonstrate the effect of changes in the parameter values.

4.2.2. The Sundqvist scheme. To show the impact of changes in the parameters in Sundqvist's parameterization scheme, the same type of situation as in subsection 4.2.1, with $w_{max}=0.5$ m/s, is chosen. The parameters in the reference case are $C_{00}=10^{-4}$, $C_1=100$ and $m_{r0}=5\cdot10^{-4}$. Fig. 5 shows the temporal change in precipitation intensity at the ground when the constant C_1 is given values between 200 and 800. As pointed out in subsection 2.2, an increase in C_1 leads to a faster approach to steady-state conditions and can be compared to a variation in E in (Ks). The vertically integrated cloud water and rain water content, expressed in mm water, are given in Table 2. From the table we see that the rain water content is constant, and that the cloud water content increases when C_1 decreases. Fig. 6 shows how the cloud water profile at steady-state varies with changes in C_1. It can be seen that variations in C_1 change the amount of cloud water, but maintain the shape of the vertical distribution. The dashed line in Fig. 6 shows the steady-state rain water profile, which is not affected by changes in C_1. This is due to the constant production of cloud water (2.14) and the absence of vertical advection.

Values of C_1 around 100 as suggested by Sundqvist (1978), thus appear to render unrealistically high values for the cloud water amount. In order to obtain more realistic values it is thus necessary to change the values of C_{00} or m_{r0} or adopt a larger value of C_1. In Table 2 the integrated cloud and rain water is given when C_{00} varies between $1.8\cdot10^{-4}$ and $1\cdot10^{-3}$. It shows that changes in C_{00} do not affect the integrated rain water amount, but that an increase in C_{00} leads to a decrease in the integrated cloud water amount. The temporal changes in the precipitation intensity, and in the cloud water profiles that we get when varying C_{00} are similar to the changes we get when C_1 is varied and are not shown. Table 2 also shows the vertically integrated cloud water content for different values of m_{r0}. From the table we see that an increase in m_{r0} leads to an increase in the cloud water, while the rain water is constant. The cloud water profiles (shown in Fig. 7) are affected in another manner than when C_1 or C_{00} are varied. An increase in m_{r0} results in an increase in the cloud water amount at all levels, but the effect is strongest at the higher levels.

4.3. *Weak convective updraft*

In this section, it will be shown how a steady-state cloud water distribution calculated from (Ks) can be simulated by (Sq) under weak convective conditions. A parabolic updraft (2.13) with $w_{max} = 0.5$ m/s will be used, and the information from subsection 4.2, about how changes in the parameter values affect the steady-state cloud water distribution, will be utilised. A steady-state distribution is calculated with (Ks) with the parameters $E = 1$, $k_2 = 0.01$ and $a = 0.5 \cdot 10^{-3}$. This cloud water profile is shown in Fig. 8 (Profile D). We then ask the question what parameter values to use in (Sq) in order to reproduce this distribution. When a value for m_{r0} has been chosen, we choose a value for either C_{00} or C_1, and then vary the other until we obtain similarity to Kessler's result. That is until the integrated cloud

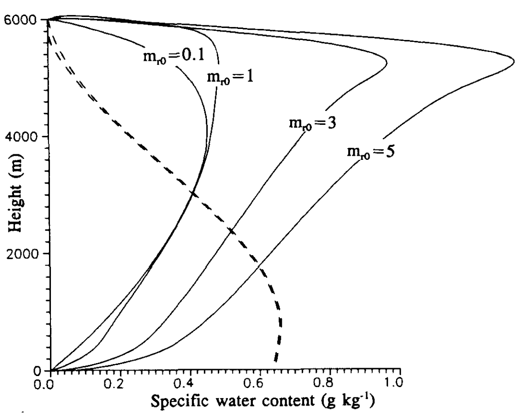

Fig. 7. As fig. 6, but for m_{r0}. Values for m_{r0} to be multiplied by 10^{-3}.

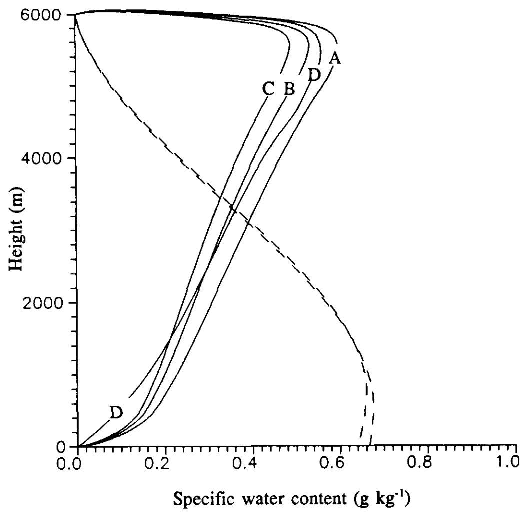

Fig. 8. Cloud water content obtained for three parameter sets in (Sq) and one in (Ks). A: (Sq), $C_{00} = 8 \cdot 10^{-4}$, $C_1 = 100$, $m_{r0} = 2 \cdot 10^{-3}$. B: (Sq), $C_{00} = 1.1 \cdot 10^{-3}$, $C_1 = 100$, $m_{r0} = 2 \cdot 10^{-3}$. C: (Sq), $C_{00} = 1.4 \cdot 10^{-3}$, $C_1 = 100$, $m_{r0} = 2 \cdot 10^{-3}$. D: (Ks), $E = 1$, $k_1 = 100$, $a = 0.5$.

water amounts are the same and the vertical distributions are most similar. Fig. 8 shows an example where $m_{r0} = 2 \cdot 10^{-3}$ and $C_1 = 100$, then C_{00} has been adjusted (Profiles A–C). Table 3 gives the total amounts of rain and cloud water for the profiles, measured in mm water at ground level. The rain water amount differs somewhat between the two parameterizations. This is due to the different ways of handling the conversion of water from cloud to rain (see subsection 4.1). Any steady-state cloud and rain water profile obtained with (Ks) can be closely simulated with (Sq), but the precipitation intensity profile with its overshooting of Kessler's approach cannot be reproduced with (Sq). The detailed difference may be less important when implemented in NWP or GCM models where much longer time steps are used. This experiment indicates that with a

Table 3. *Vertically integrated cloud and rain water content for the profiles in Fig. 8, measured in mm*

Profile	*A*	*B*	*C*	*D*
Cloudwater	1.96	1.72	1.56	1.73
Rainwater	2.58	2.58	2.58	2.55

suitable choice of parameter values, the simpler scheme (Sq) is able to reproduce most of the patterns obtained with the more detailed microphysics in (Ks). Strong updrafts (5–10 ms^{-1}) have also been considered with test runs showing close similarity between the two schemes. Therefore we present no results here but just refer to Kessler (1969).

4.4. *Weak vertical updraft; stratiform type*

In the calculations of this section, stratiform conditions are simulated. This is done in the same manner as in the previous cases, except for another updraft speed, namely $w_{max} = 0.1$ m/s. The results from (Sq) is obtained with the parameter values recommended for stratiform conditions, $C_{00} = -10^{-4}$, $C_1 = 100$ and $m_{r0} = 0.3 \cdot 10^{-3}$. Profiles of the cloud water content at different stages of the development shows that the increase in the cloud water content is almost evenly distributed with height, and it is only when steady-state is reached (after 6 h), vertical advection and/or outwash at low levels has any effect at all. The precipitation from (Ks), has a slow approach towards its steady-state value. Test runs have shown that this is occurring because the time and height resolution is coarse. When applying (Ks) we find that the outwash at lower levels affects the profiles of the cloud water content notably, and the total steady-state cloud water content with (Ks) is much lower than with (Sq). This is a function of the value Kessler suggests for the efficiency of the collision-coalescence term, namely $E = 1$. Test runs show that a decrease in E leads to profiles more like the ones from (Sq). (Ks) was originally applied to a convective situation (the parameter values are in accordance with that), and that has to be considered as an explanation when results from (Ks) and (Sq) have large differences.

Obviously, the treatment of stratiform clouds is very different for the two schemes when the given parameters are applied, but the results from both schemes lie inside the range of observation statistics. Based on statistical values from large samples, Matveev (1984) reports water content of stratiform clouds varying from 0.05 to 0.8 g/kg. Curry et al. (1989) have used satellite micro-wave measurements to display rain rate as a function of the liquid water path (sum of integrated cloud and precipitation water in the column), and have found that liquid water paths from 200 to 800 g m^{-2} corresponds to rain fall rates from 0 to 4 mm h^{-1}. Calculating the liquid water path of the steady-state distributions, we find that the steady-state (Sq) profile had a liquid water path of 2600 g m^{-2}, and that the (Ks) profile had a liquid water path of 1750 g m^{-2}. The corresponding rainfall rates are 3 mm h^{-1} in both cases. The water paths from (Sq) and (Ks) are thus rather large when compared to the measured precipitation rates and the matching liquid water paths, indicating that both schemes should employ parameter values that yield larger conversion rates.

4.5. *Evaporation and development from subsaturation*

When the initial conditions are subsaturated, an increase in humidity is necessary before condensation can take place. Saturation will first be reached at the layer where maximum updrafts takes place. The coexistence of clouds and unsaturated layers makes it necessary to include the effect of evaporation of rain water in the calculations. This is done with an additional microphysical term in the continuity eqs. (2.1) and (2.2).

Except for the initial conditions and the inclusion of evaporation, the calculations in this section are the same as in subsection 4.3. We have chosen to deal with subsaturation in the same manner as Kessler. The parameter $m(z, t)$ is a measure of both cloud water content and humidity; a negative $m(z, t)$ means the amount of water vapour necessary to reach saturation. The evaporation is described by Kessler by the following term.

$$\begin{aligned} &\mathrm{EP} = k_3 N_0^{7/20} m(z, t)(\rho M)^{13/20}, \\ &k_3 = 1.72 \cdot 10^{-4}, \qquad \text{when} \quad m < 0, \\ &k_3 = 0, \qquad \text{when} \quad m \geqslant 0. \end{aligned} \tag{4.1}$$

Sundqvist uses the following formulation for the evaporation effect:

$$\begin{aligned} &\mathrm{EP} = k_{\mathrm{E}}(U - 1)\, \tilde{P}^{1/2}, \\ &k_{\mathrm{E}} = 7 \cdot 10^{-5}, \qquad \text{when} \quad m < 0, \\ &k_{\mathrm{E}} = 0, \qquad \text{when} \quad m \geqslant 0, \end{aligned} \tag{4.2}$$

where U is the relative humidity; $U = 1$ corresponding to 100% relative humidity. The size of the constant k_{E} in this calculation is chosen so that (Sq) gives the most similar cloud water profile

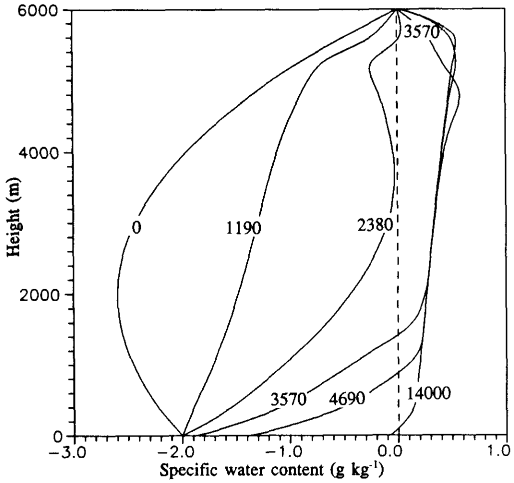

Fig. 9. Cloud water/humidity-deficit profiles calculated with the Sundqvist scheme when $k_E = 7 \cdot 10^{-5}$.

when compared to (Ks) (only the profile from (Sq) is shown). Sundqvist (1988) suggests $k_E = 10^{-5}$, but when this value is used the development towards a saturated atmosphere, is much slower than in the calculation performed with (Ks).

The other parameter values are the same as in the reference case (subsection 4.3). The results from a run with (Sq) when $k_E = 7 \cdot 10^{-5}$ is shown in Fig. 9. The effect of the evaporation term is easiest to see at ground level. There is no production of cloud water from vapour at this level since $w = 0$. So any increase in $m(0, t)$ is caused by evaporation of precipitation. At the levels just above the ground the evaporation term has the effect of increasing the humidity at the expense of the precipitation water content, and thereby modifying both the profile of $m(z, t)$ and the profile of the rain water content. At higher levels the evaporation is much less important because the humidity deficit when precipitation is produced is small, that is $m \approx 0$, and as a consequence $\mathrm{EP} \approx 0$ at these levels.

5. High/cold clouds

Kessler (1969) does not consider cases with cold clouds. He merely mentions that the process of growth of tiny ice particles to precipitation size is represented by the auto-conversion term, i.e., eq. (2.4), and the growth of hail be accretion by the collision-coalescence term (2.7). Other schemes with bulk representation of cold clouds have been proposed (i.e., Star and Cox 1985), but only a few has to our knowledge been incorporated into NWP models. Therefore we have chosen only to test the scheme for cold or high cirrus clouds as suggested in Sundqvist (1988). The particular descriptions have been slightly revised and it is the latter ones that are employed below (Sundqvist, personal communication).

For temperatures above 273 K, the warm cloud parameterization (2.8) is used. When the temperature is below 273 K we modify C_0 and m_r with temperature dependent parameters/functions. Hence

$$C_0 = C_{00} F_{13}, \tag{5.1}$$

$$m_r = (m_{r0} f_{mr})/F_1, \tag{5.2}$$

where

$$F_{13} = F_1(1 + C_2 f_{BF}) \times \left[1 + C_3 \frac{(1 - f_{mr})}{f_{mr}}\right], \quad C_2 \approx 4.0, \quad C_3 = 0.12, \tag{5.3}$$

and

$$f_{mr} = 1.33 \exp(-[0.066(T - T_0)]^2), \quad f_{mr} \leqslant 1. \tag{5.4}$$

F_1 is given by (2.10). The function f_{BF} is introduced to simulate Bergeron–Findeisen effects

$$f_{BF} = f_i^{(\mathrm{mod})}(1 - f_i)\, S, \tag{5.5}$$

where S is the difference in saturation value of vapour density over water and ice and f_i is the probability for existence of ice crystals. (f_i is approximated with an exponential function dependent on the temperature varying from 0 at 268 K to 1 at 233 K.)

The factor in (5.3) including C_3 is meant to introduce characteristics of low temperature clouds. f_{mr} is a function for modification of m_r for temperatures beneath 273 K. A modified, or total, probability of ice in a layer, $f_i^{(\mathrm{mod})}$, is depending on the fraction $(\tilde{P}_i/\tilde{P}_{\mathrm{tot}})$ of ice crystals in the precipitation coming into the layer in question.

$$f_i^{(\mathrm{mod})} = f_i + (1 - f_i) \frac{\tilde{P}_i(\mathrm{in})}{\tilde{P}_{\mathrm{tot}}(\mathrm{in})}. \tag{5.6}$$

The amount of ice/snow of the total rate of precipitation, at the base of a model layer, is

$$\tilde{P}_i(\text{out}) = \tilde{P}_i(\text{in}) + f_i^{(\text{mod})} P \rho \, \Delta z. \tag{5.7}$$

For $236 < T < 250$, F_{13} is given by (5.3), while for $236 > T > 232$, (5.8) is used

$$F_{13} = 0.25 F_1 [F_3(T - 232) + 5(236 - T)], \tag{5.8}$$

and for $T < 232$, (5.9) is adopted

$$F_{13} = 5. \tag{5.9}$$

For $T < 250$, f_{mr} is calculated from

$$f_{\text{mr}} = 0.075 \left(1.07 \pm \frac{y}{1+y} \right)$$

(minus sign for $T < 232$ K)

$$y = x \left(1 + x + \frac{4}{3} x^2 \right), \qquad x = \frac{|T - 232|}{18}. \tag{5.10}$$

The functions describing $f_i(T)$, $f_{\text{mr}}(T)$, $S(T)$ and $f_{\text{BF}}(T)$, are taken from Sundqvist (1988). The temperature profile used in the computations is linear and decreases from 280 K at ground to 224 K at 6000 m. It has been chosen in order to easier demonstrate the effect under consideration. A temperature profile like this is of course conditionally unstable, but this can be disregarded because there is no dynamic feedback in the model. In Fig. 10 the levels where a shift in parameterization takes place is indicated.

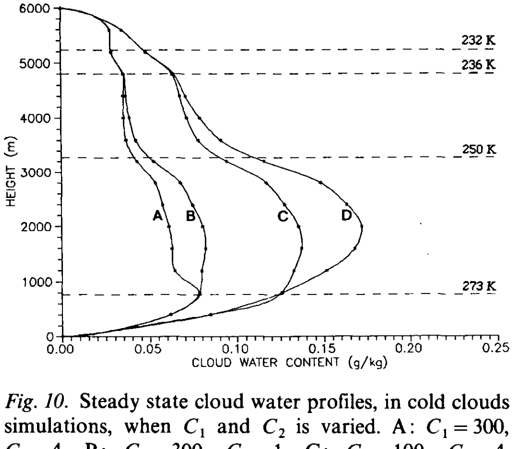

Fig. 10. Steady state cloud water profiles, in cold clouds simulations, when C_1 and C_2 is varied. A: $C_1 = 300$, $C_2 = 4$. B: $C_1 = 300$, $C_2 = 1$. C: $C_1 = 100$, $C_2 = 4$. D: $C_1 = 100$, $C_2 = 1$.

When a cold atmosphere is considered we have the change constants A and B in the condensation function $G(z)$ given in (2.14). As a consequence of a lower vapour content, a more realistic condensation rate is obtained with $A = 3 \cdot 10^{-7}$ and $B = 3 \cdot 10^{-11}$. A few steady-state profiles obtained with different parameter values are shown in Fig. 10 ($C_{00} = 1 \cdot 10^{-4}$ and $m_{r0} = 2 \cdot 10^{-3}$ are constant). When $C_1 = 300$ and $C_2 = 4$ we see that a very efficient conversion of cloud into precipitation takes place at all levels. Decreasing C_2 to $C_2 = 1$, we have an increase in cloud water at the levels where T is between 250 and 273 K. Changing C_1 and C_2 to $C_1 = 100$ and $C_2 = 4$, implies that an increase in cloud water takes place at all levels. When $C_1 = 100$ and $C_2 = 1$, we see that the cloud water content is further increased at the levels corresponding to $250 < T < 273$.

Matveev (1984) has investigated numerous cases with cold clouds, both stratiform and convective. The statistical data concerning cloud water amount as a function of temperature and cloud type can be used to judge if the computed values are realistic or not. But due to the large standard deviations in all the measurements they only provide an indication. If we look at the temperature interval between 250 and 255 K in convective clouds, corresponding to around 3200 m in the presented figures, the measured specific water content has a value of 0.09 ± 0.04 g/kg. We see that all the computed values lie within the deviation of this value. The results also agree with Heymsfield and Donner (1990).

6. Conclusions

We have compared some of the features of Kessler's (1969) and Sundqvist's (1988) schemes for parameterization of cloud and precipitation formation. It is found that Sundqvist's parameterization scheme with a suitable choice of parameter values can give results very similar to those of Kessler's scheme. For all the examples studied, it has been verified that the choice of parameters is very important, and for some of the cases it is indicated that the parameter values, which have been suggested originally, should be changed. On the basis of this study, new values for the parameters in Sundqvist's parameterization scheme can be proposed. In the comparison of the two schemes, it is pointed out that in some of the cases, the two schemes give very different results when the original parameter values are used.

We have not had measurements from specific cases available for comparison of the results of this study. Statistics from observations of cloud water content has been utilized to check if the model results appear to be realistic. Those observations indicate that in some of the cases both schemes have too much cloud water when related to the corresponding precipitation rates. This was observed for both schemes in the case of stratiform clouds, and for Sundqvist's scheme, when applied to cold clouds. It has been shown that the spatial resolution is important for the accuracy of the results when Kessler's parameterization is applied in the computations, while Sundqvist's scheme is less sensitive when the resolution is made coarser. Kessler's scheme was especially sensitive to changes in the resolution when evaporation was included.

The inclusion of three interacting micro-physical terms in (Ks) (where two of them contain both the prognostic variables) caused pronounced oscillations. This happened with the Kessler scheme when the spatial resolution was too low, and resulted in unrealistic oscillations of the cloud and rain water in time. The oscillations can of course be suppressed with an averaging in time and space, but this affects the results strongly. The ideal way to diminish those fictitious effects is to increase the resolution. It may be an important aspect that the Kessler scheme needs a higher resolution than the Sundqvist scheme. This favours the Sundqvist scheme for use in large prediction models where the number of levels is restricted in the interest of saving computation time.

7. Acknowledgments

I would like to thank professor Hilding Sundqvist at Stockholm University and colleagues at the University of Bergen for helpful discussions, and for a motivational contribution to my work.

8. Appendix

List of symbols

m	specific cloud water content
M	specific rain water content
V	fallspeed of raindrops
w	vertical wind velocity
w_{max}	maximum updraft speed
ρ	air density
ρ_0	air density at ground with standard atmosphere
k	standard atmosphere constant
G	condensation function
Q_s	specific saturation water content
N_0	number of drops
H	height of updraft column
k_1	constant in (Ks), $k_1 \approx 0.01$
a	constant (treshold value) in (Ks), $a \approx 0.5 \cdot 10^{-3}$
k_2	constant in (Ks), $k_2 = 6.96 \cdot 10^{-4}(10^3\rho_0)^{7/8} N_0^{1/8}$
E	efficiency of the collision-coalescence process
C_0	constant in (Sq)
C_{00}	constant in (Sq)
m_r	constant in (Sq)
m_{r0}	constant in (Sq)
C_1	constant in (Sq)
P	production rate of precipitation at a single level
$\tilde{P}(z)$	total production rate of precipitation above z
$\tilde{P}_i(z)$	total production rate of ice crystals above z
F_1	modifying factor in (Sq)
F_3	modifying factor in (Sq) cold clouds scheme
C_2, C_3	constants in (Sq) cold clouds scheme
f_{mr}	function for modification of m_r for $T < 273$ K
F_{BF}	modifying factor in (Sq) cold clouds scheme (accounts for the Bergeron Findeisen effects)
f_i, $f_i^{(mod)}$	probability for existence of ice in a layer
S	difference in saturation value of vapour density over water and ice
k_3	constant in (Ks) for evaporation
k_E	constant in (Sq) for evaporation

Reference parameter values

Convective case

(Sq): $C_1 = 100$, $C_{00} = 1.1 \cdot 10^{-3}$, $m_{r0} = 2 \cdot 10^{-3}$
(Ks): $E = 1$, $k_1 = 0.01$, $a = 0.5$ (g/kg)

Stratiform case

(Sq): $C_1 = 100$, $C_{00} = 10^{-4}$, $m_{r0} = 0.3 \cdot 10^{-3}$

(Ks): $E = 1$, $k_1 = 0.01$, $a = 0.3$ (g/kg)

Evaporation

(Sq): $k_E = 7 \cdot 10^{-5}$

(Ks): $k_3 = 1.72 \cdot 10^{-4}$

REFERENCES

Charlock, T. P. 1982. Cloud optical feedback and climate stability in a radiative convective model. *Tellus 34*, 245–254.

Charlock, T. P. and Ramanathan, V. 1985. The albedo field and cloud radiative forcing produced by a general circulation model with internally generated cloud optics. *J. Atmos. Sci. 42*, 1408–1429.

Curry, J. A., Ardeel, C. D. and Tian, L. 1989. Liquid water content and precipitation characteristics of stratiform clouds as inferred from satellite microwave measurements. *J. Geophys. Res. 95*, 16659–16671.

Heiden, T. and Kahlig, P. 1988. An analytic solution of convective precipitation. *Annales Geophysicae 6*, 225–230.

Heymsfield, A. J. and Donner, L. J. 1990. A scheme for parameterizing ice-cloud content in general circulation models. *J. Atmos. Sci. 47*, 1865–1877.

Kristjànsson, J. E. 1991. Cloud parameterization at different horizontal resolutions. *Quart. J. Roy. Met. Soc.*, in press.

Kessler, E. 1969. On the distribution and continuity of water substance in atmospheric circulation. *Met. Monograph 10, 32*, American Meteorological Society, Boston, USA.

Lax, P. D. 1954. Weak solutions of nonlinear hyperbolic equations and their numerical computation, *Commun. Pure Appl. Math. 7*, 159–193.

Matveev, L. 1984. *Cloud dynamics*. D. Reidel Publishing Company. Dordrecht, Germany.

McMurdie, L. A. and Katsaros, K. B. 1985. Atmospheric water distribution in a mid-latitude cyclone observed by the Seasat Scanning Multichannel Microwave Radio-meter. *Mon. Wea. Rev. 113*, 584–589.

Roeckner, E., Schlese, U., Biercamp, J. and Loewe, P. 1987. Cloud optical depth feedbacks and climate modelling. *Nature 329*, 138–140.

Rogers, R. R. 1979. *A short course in cloud physics*, 2nd edition (International series in natural philosophy) Pergamon international library. Oxford, UK.

Star, D. O'C. and Cox, S. K. 1985. Cirrus clouds. Part I: A cirrus cloud model. *J. Atmos. Sci. 42*, 2663–2668.

Sulakvelidze, G. K. 1969. *Rainstorm and hail*. Israel program for scientific translations, Jerusalem, Israel.

Sundqvist, H. 1978. A parameterization scheme for non-convective condensation including prediction of cloud water content. *Quart. J. Roy. Met. Soc. 104*, 677–690.

Sundqvist, H. 1988. Parameterization of Condensation and Associated Clouds in Models for Weather Prediction and General Circulation Simulation. In: *Physically-based modelling and simulation of climate and climatic change* (ed. M. E. Schlesinger), Reidel, Dordrecht, 433–461.

Sundqvist, H., Berge, E. and Kristjánsson, J. E. 1989. Condensation and cloud parameterization studies with a mesoscale NWP model. *Mon. Wea. Rev. 117*, 1641–1657.